

Gas and Vapor Solubility in Cross-Linked Poly(ethylene Glycol Diacrylate)

Haiqing Lin and Benny D. Freeman*

Department of Chemical Engineering and Center for Energy and Environmental Resources,
University of Texas at Austin, 10100 Burnet Road, Austin, Texas 78758

Received June 9, 2005; Revised Manuscript Received July 10, 2005

ABSTRACT: Polymers containing poly(ethylene glycol) (PEG) have been investigated for CO₂ removal from mixtures with light gases such as CH₄, N₂, and H₂ because of the good affinity of PEG for CO₂. In this study, the solubilities of CO₂ and several hydrocarbons (CH₄, C₂H₄, C₂H₆, C₃H₆, and C₃H₈) were determined as a function of gas fugacity (i.e., pressure) at temperatures ranging from −20 °C to 35 °C in cross-linked amorphous poly(ethylene glycol) diacrylate (XLPEGDA), which was prepared by UV photopolymerization of poly(ethylene glycol) diacrylate and contains about 82 wt % PEG. Sorption isotherms were described using the Flory–Huggins model. Unlike sorption in nonpolar rubbery polymers, solubility of gases such as CO₂ and olefins in polar XLPEGDA do not vary systematically based on parameters used conventionally to characterize gas condensability such as critical temperature (T_c) or $(T_c/T)^2$, so a new model is proposed to correlate the data. CO₂ exhibits the lowest Flory–Huggins interaction parameter (i.e., χ) values among all of the penetrants considered, indicating favorable interactions with XLPEGDA. Although gas solubility at a given pressure generally increases as temperature decreases, χ values increase with decreasing temperature for all penetrants except CO₂. These results reflect the interplay between increases in penetrant condensability as temperature decreases, which tend to increase solubility, and increases in the unfavorable interactions between the gas and polymer segments (reflected in the increased χ values) as temperature decreases, which tend to reduce solubility. χ values for CO₂ in XLPEGDA decrease with decreasing temperature, which is another indication of the affinity between CO₂ and XLPEGDA. The following example illustrates the effect of temperature on intermolecular interactions: CO₂/C₂H₆ solubility selectivity at infinite dilution increases from 2.7 to 6.6 as temperature decreases from 35 °C to −20 °C, even though these two penetrants have almost the same condensability as characterized by T_c . Furthermore, gas solubility values in XLPEGDA are very similar to those in amorphous PEG at infinite dilution and 35 °C, suggesting that the PEG linkages in XLPEGDA dominate its sorption properties.

Introduction

Gas separation using polymeric membranes has grown significantly since the 1980s, and polymer membranes now compete successfully with conventional gas separation technologies, such as cryogenic distillation, absorption, and pressure-swing adsorption (PSA) in certain applications, such as hydrogen recovery from nitrogen in ammonia purge gas streams, hydrogen separation from methane in refinery off-gases and hydrogen removal from carbon monoxide in synthesis gas, nitrogen enrichment from air, and removal of acid gases (e.g., CO₂) from natural gas.^{1,2}

Gas transport through a nonporous membrane can be characterized as a solution–diffusion process, and the fugacity and thickness normalized flux, or permeability (P_A), is often expressed as follows³

$$P_A = D_A S_A \quad (1)$$

where D_A is the average effective diffusivity of the gas in the film, and S_A is the gas solubility coefficient. The ideal selectivity of a membrane for gas A over gas B is the ratio of their pure gas permeabilities⁴

$$\alpha_{A/B} = \frac{P_A}{P_B} = \left[\frac{D_A}{D_B} \right] \left[\frac{S_A}{S_B} \right] \quad (2)$$

where D_A/D_B is the diffusivity selectivity and S_A/S_B , is

* Corresponding author. Tel: +01-512-232-2803. Fax: +01-512-232-2807. E-mail: freeman@cche.utexas.edu.

the solubility selectivity. Diffusivity selectivity favors transport of smaller penetrants and becomes more significant as the size-sieving ability of the polymer matrix increases and as the size difference between the gases increases. In contrast, solubility selectivity favors more condensable (often larger) penetrants and is affected by the relative affinity between the penetrants and the polymer matrix and the condensability difference between the gases.⁴

In general, solubility selectivity is often observed to be relatively insensitive to polymer structure because it typically depends most strongly on relative penetrant condensability, which is independent of the polymer.⁵ In contrast, diffusivity selectivity changes substantially from polymer to polymer and depends sensitively on polymer-dependent parameters such as the polymer fractional free volume and the glass transition temperature.^{5,6} Commercially used membranes achieve high separation factors mainly from diffusivity selectivity, and they are generally glassy polymers with high glass transition temperatures (T_g), such as polysulfone ($T_g \approx 190$ °C)⁷ and polyimides ($T_g \approx 300$ °C).⁸ The resulting rigid polymer chains, coupled with the relatively low free volume of these materials, sieve gas molecules based strongly on size differences among the gas molecules.⁸

Recently, some applications began to require the removal of larger molecules from mixtures with smaller molecules.^{1,6} For example, volatile organic compounds (e.g., vinyl chloride monomer, propylene, ethylene, gasoline, Freons) need to be recovered from mixtures

with air or nitrogen.⁹ Of particular interest to this study is the removal of carbon dioxide from mixtures with hydrogen, an important basic chemical and a potential energy carrier for fuel cells.¹⁰ Currently, H₂ is produced by steam reforming of hydrocarbons followed by the water gas shift reaction.² Such H₂ always contains CO₂ as a byproduct, and often the CO₂ must be removed to increase the purity of the hydrogen product. In these separations, larger molecules (e.g., propylene in propylene/nitrogen separations¹ and CO₂ in CO₂/H₂ separations¹¹) are often the minor components in the feed and, therefore, separation using membranes that are more permeable to larger molecules (so-called reverse-selective membranes) could require less membrane area and, in turn, lower capital cost than conventional membranes.¹² Additionally, some product gases, such as hydrogen, are required at high pressure for further use, and reverse-selective membranes can provide significant economic benefits because they keep the H₂ at high pressure while removing the CO₂ contaminant. Reverse-selective membrane materials separate molecules based strongly on solubility selectivity because larger molecules are often more condensable and, thus, more soluble in polymers than smaller molecules. Furthermore, because gas sorption in polymers depends sensitively on temperature, it is critical to understand the effect of temperature on gas solubility to achieve the best separation performance using reverse-selective membranes.

Solubility selectivity of CO₂ over light gases can be improved by introducing polar groups into the polymer matrix because CO₂ has a quadrupolar moment that interacts favorably with polar groups.¹³ On the basis of a recent review of interactions between liquids containing various polar groups and CO₂, polar ether oxygens were identified as exhibiting highly favorable interactions with CO₂, and poly(ethylene oxide) (PEO) (or, equivalently, poly(ethylene glycol) (PEG)) based materials appear to be attractive candidates for separations involving CO₂.¹³ Many PEO-containing materials have been studied for CO₂ removal from light gases such as H₂.^{11,14–21} Previously, gas solubility, diffusivity, and permeability have been reported in PEO, which is a semicrystalline polymer that is reverse-selective, at least with respect to CO₂ transport over H₂.¹⁹ PEO exhibits relatively high CO₂/H₂ and CO₂/CH₄ permeability selectivity because of solubility selectivity favoring CO₂ in these gas pairs. Additionally, CO₂/H₂ and CO₂/CH₄ permeability selectivities increase as temperature decreases.¹⁹ However, because of the high crystallinity in PEO (71 vol %), PEO exhibits rather low gas permeability and solubility.¹⁹ Therefore, it would be useful to prepare amorphous materials that contain high concentrations of ethylene oxide units. We have reported calorimetry data for cross-linked poly(ethylene glycol diacrylate) (XLPEGDA); this material contains about 82 wt % EO and does not crystallize at temperatures as low as –20 °C.²² This paper discusses the effect of temperature and pressure on gas solubilities of CO₂ and several hydrocarbons (CH₄, C₂H₆, C₂H₄, C₃H₈, and C₃H₆) in XLPEGDA, and it compares solubility behavior in amorphous XLPEGDA with that in semicrystalline PEO at 35 °C. A companion paper reports the effect of temperature and pressure on gas permeability and diffusivity in XLPEGDA.²³

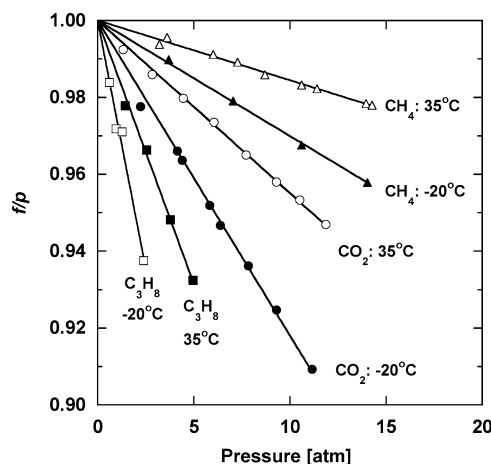


Figure 1. Effect of pressure and temperature on the ratio of pure gas (CH₄, CO₂, and C₃H₈) fugacity to the corresponding pressure.

Background. Gas solubility, S_A , is given by^{3,4,24}

$$S_A = \frac{C}{f} \quad (3)$$

where C is the concentration of gas dissolved in the polymer when the fugacity of the gas phase in contact with the polymer is f . Instead of pressure, fugacity is used in this study to appropriately account for gas-phase nonidealities,²⁴ which can become significant at low temperature (e.g., –20 °C) for penetrants such as CO₂. For example, Figure 1 presents the ratio of pure gas fugacity to pressure for CH₄, CO₂, and C₃H₈ as a function of pressure at 35 °C and –20 °C. The gas is ideal if $f/p = 1$ and becomes more nonideal as f/p deviates further from unity. The equation used to calculate fugacity is presented in the Appendix. As temperature decreases, the gas-phase becomes more nonideal. Nonideal behavior is more significant for CO₂ and C₃H₈ than for gases such as CH₄. For example, CO₂ exhibits an f/p value of 0.91 at –20 °C and 12 atm, whereas CH₄ exhibits a value of 0.96 at similar conditions. C₂H₄ and C₂H₆ exhibit nonideal behavior similar to that of CO₂, and C₃H₆ behaves similar to C₃H₈.

Gas sorption isotherms were fit to the Flory–Huggins model³

$$\ln \frac{f}{f_{\text{sat}}} = \ln \phi_2 + (1 - \phi_2) + \chi(1 - \phi_2)^2 \quad (4)$$

where f_{sat} is the penetrant saturation fugacity at the temperature of interest, χ is the Flory–Huggins interaction parameter, and ϕ_2 is the volume fraction of penetrant dissolved in the polymer matrix. f_{sat} is calculated using eq A3 from the Appendix and saturation vapor pressure data from the DIPPR database.²⁵ Other factors, such as the influence of cross-link density or the amount of water in the prepolymer solutions, were shown to have a negligible impact on gas sorption, so they are not included in this analysis.²² The gas volume fraction, ϕ_2 , can be written as²⁶

$$\phi_2 = \frac{(C/22\,414)\bar{V}_2}{1 + (C/22\,414)\bar{V}_2} \quad (5)$$

Table 1. Physical Properties of Penetrants Including Critical Volume (V_c), Estimated Partial Molar Volume at 35 °C (\bar{V}_2), Critical Temperature (T_c), and Saturation Vapor Fugacity at 35 °C (f_{sat})

gas	size		condensability ^a	
	V_c ⁷² (cm ³ /mol)	\bar{V}_2 ³² (cm ³ /mol)	T_c ⁷² (K)	f_{sat} ²⁵ (atm)
CO ₂	93.9	45	304	53 ^a
CH ₄	99.2	46	191	351 ^a
C ₂ H ₄	130.4	57	282	51 ^a
C ₂ H ₆	148.3	61	305	34 ^a
C ₃ H ₆	181.0	73	365	12
C ₃ H ₈	203.0	80	370	10

^a f_{sat} values are estimated using saturation vapor pressure values from the DIPPR database.²⁵ The f_{sat} values of CO₂, CH₄, C₂H₄, and C₂H₆ are hypothetical because the values of saturation vapor pressure for these penetrants were extrapolated using empirical equations provided by the DIPPR database.

where \bar{V}_2 is the penetrant partial molar volume (cm³/mol) in the polymer.

Experimental Section

Materials. Chemical purity (99%) cylinders of methane, ethane, ethylene, propane, and propylene were received from Air Liquide America Corporation (Houston, TX), and 99.9% carbon dioxide was received from Air Gas Southwest Inc. (Corpus Christi, TX). All gases were used as received. Table 1 records the physical properties of the gases of interest. Poly(ethylene glycol) diacrylate (CH₂=CHCOO(CH₂CH₂O)₁₄OCCH=CH₂; MW = 743), poly(propylene glycol) diacrylate (CH₂=CHCOO(CH₂CHCH₃O)₁₃OCCH=CH₂; MW = 900), hexane, dodecane, chloroform, and 1-hydroxycyclohexyl phenyl ketone (HCPK) were purchased from Aldrich Chemical Co. (Milwaukee, WI). All solvents had a purity of at least 99%. All chemicals were used as received unless otherwise indicated. Ultrapure water was produced by a Milli-Q water purification system (Millipore Corporation, Bedford, MA).

Polymer Synthesis and Film Preparation. The prepolymer solution to prepare XLPEGDA was prepared by adding 0.1 wt % initiator (i.e., HCPK) to PEGDA. After stirring, the solution was mixed with ultrapure water to form a solution containing 80 wt % PEGDA. The solution was sandwiched between two quartz plates equipped with spacers of uniform thickness to control film thickness. The solution was polymerized by exposure to UV light in a UV cross-linker (Model FB-UVXL-1000, Fisher Scientific) for 90 s at 312 nm and 3.0 mW/cm². The resulting solid films were three-dimensional networks (i.e., gels) and contained a negligible amount of low molecular weight polymer (i.e., sol) that was not bound to the network.²² Any sol or unreacted cross-linker was removed by immersing the films in a large amount of ultrapure water for at least 5 days. The water was replaced with fresh ultrapure water daily. The final film thicknesses ranged from 200 to 500 μ m. Cross-linked poly(propylene glycol) diacrylate films were prepared using conditions similar to those of XLPEGDA, except that 20 wt % chloroform was used (instead of water) in the prepolymer solution.

Sorption Measurements. Gas solubility was determined using a dual-volume, dual-transducer apparatus based on the barometric, pressure-decay method.²⁷ A general procedure for this experiment has been described elsewhere.^{28,29} Blank experiments were performed for all of the gases at the temperatures of interest, with nonsorbing volumes (e.g., stainless steel spheres) added to the sample cell. Ideally, the gas solubility estimated from these experiments should be zero because these nonporous spheres sorb a negligible amount of gas. However, because of uncertainties in the pressure readings and the sorption cell volume, a small nonzero value was typically obtained. In these gas sorption studies, the polymer sample had a volume similar to that of the nonsorbing calibration spheres, and the pressure increase sequence in the experiments with polymer samples was similar to that used in the blank experiments for different gases at different

Table 2. Physical Properties of XLPEGDA²²

density (g/cm ³)	FFV ^a	T_g ^b (°C)	water uptake (g H ₂ O/g polymer)	cross-link density (mol/cm ³) ^c
1.188	0.117	−42	0.72	1.9×10^{-3}

^a Fractional free volume was estimated using density and group contribution theory.⁴² ^b Glass transition temperature from differential scanning calorimetry. ^c Estimated using the Peppas–Lucht model and equilibrium water uptake results.²²

temperatures. The solubility values obtained in this way were compared to those obtained from the blank experiments. The differences between these two series of results are reported as the true gas sorption in the polymer. A general rule of thumb used to judge the validity of the data is that the gas solubility values obtained using the polymer samples should be at least 10 times the values from the blank experiments. In this study, the criterion was met for all penetrants except CH₄, which exhibited the lowest solubility. For example, at 0 °C, the hypothetical CO₂ solubility from the blank experiments was −0.06 cm³(STP)/(cm³ atm), whereas the measured CO₂ solubility in polymer samples was about 3.2 cm³(STP)/(cm³ atm). In contrast, the hypothetical CH₄ solubility was −0.04 cm³(STP)/(cm³ atm), and the measured CH₄ solubility was 0.13 cm³(STP)/(cm³ atm). This situation was particularly severe for H₂, and because its solubility was so low in these polymers, it was not possible to obtain reliable estimates of H₂ solubility. Similarly, the solubility of N₂ was also too low to be measured accurately.

Results and Discussion

Characterization of Polymer Samples. Table 2 provides the physical properties of the XLPEGDA films used in this study. These results have been reported elsewhere, along with the measurement or calculation method.²² The polymer is amorphous at room temperature, and it does not show any crystallization or melting peaks in the temperature range from −90 to 0 °C as characterized by differential scanning calorimetry (DSC).²² Therefore, over the temperature range considered (i.e., from −20 °C to 35 °C), the polymer sample is considered to be amorphous.

Gas Sorption, Solubility, and Interaction Parameter. Sorption isotherms for CH₄, C₂H₄, C₂H₆, CO₂, C₃H₆, and C₃H₈ in XLPEO are presented as a function of temperature in Figure 2a–f. The detailed values are summarized in Table 3. For low sorbing penetrants, such as CH₄ at all temperatures studied and C₂H₆ at 35 °C, the isotherms are linear. For highly sorbing penetrants, such as CO₂, C₂H₄, C₃H₆, and C₃H₈ at any temperature studied and C₂H₆ at temperatures lower than 35 °C, the isotherms are slightly convex to the fugacity axis.

Figure 3a and b presents CO₂ and C₂H₄ solubility as a function of temperature and fugacity, respectively. At higher temperatures, such as 298 and 308 K, the CO₂ and C₂H₄ solubility coefficients are essentially independent of fugacity. However, at lower temperatures, such as 253 K, their solubility increases with increasing fugacity. For example, at 253 K, the CO₂ solubility coefficient increases by 30%, from 5.6 to 7.3 cm³(STP)/(cm³ atm), as CO₂ fugacity increases from 0.8 to 9.9 atm.

All of these isotherms can be described by the Flory–Huggins model (i.e., eq 4) with appropriate values of the Flory–Huggins interaction parameter, χ . In general, χ depends on penetrant volume fraction and temperature, as described by the following empirical model^{30,31}

$$\chi = \chi_0 + \frac{\chi_1}{T} + \chi_2(1 - \phi_2) \quad (6)$$

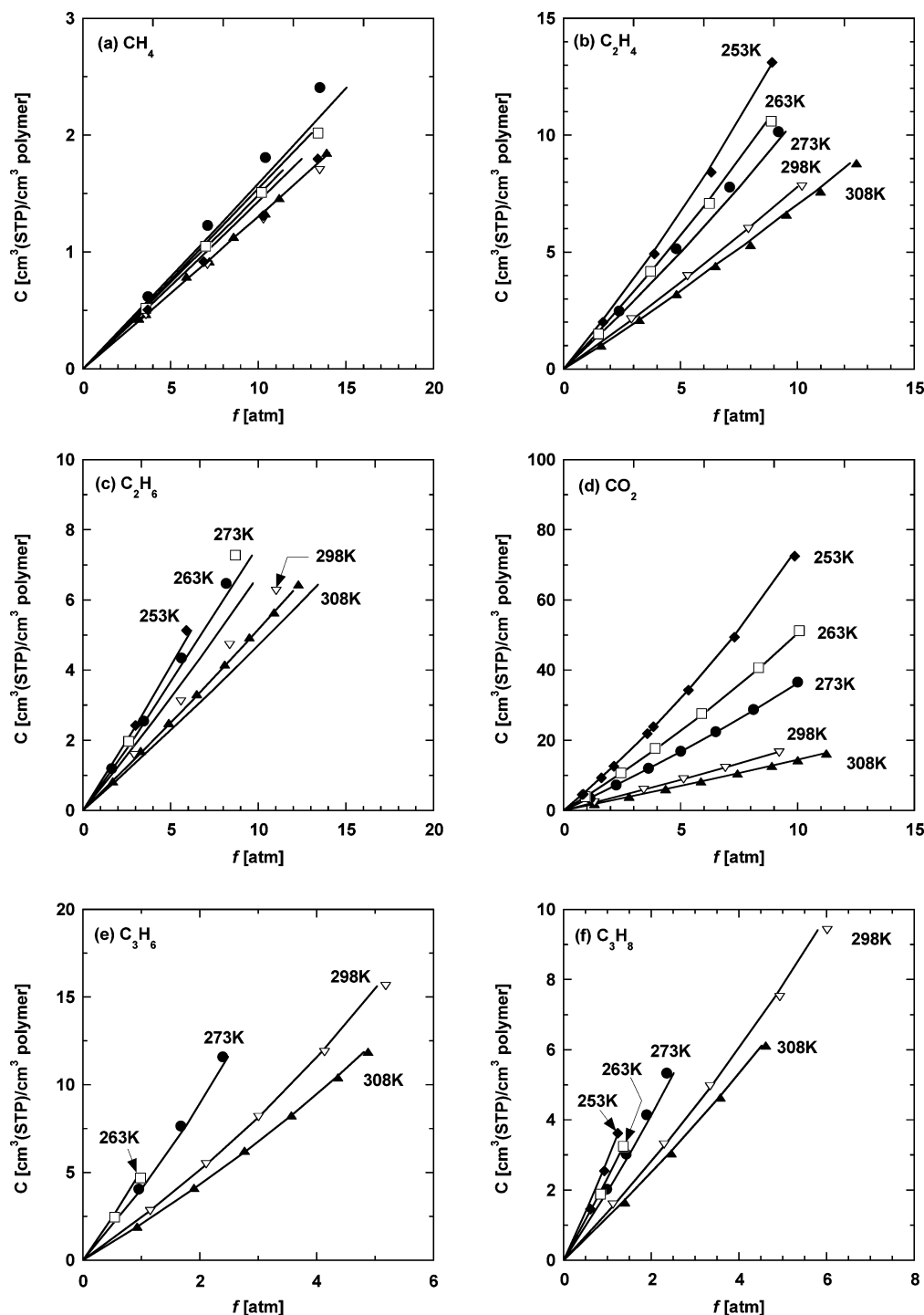


Figure 2. Effect of temperature on sorption isotherms in XLPEGDA. $T = 308 \text{ K}$ (\blacktriangle), 298 K (∇), 273 K (\bullet), 263 K (\square), and 253 K (\blacklozenge). The lines and curves through the data are based on eqs 4–6. The best-fit values of the adjustable constants, χ_0 , χ_1 , and χ_2 , are recorded in Table 4.

where χ_0 , χ_1 , and χ_2 are adjustable constants. By adjusting these constants, the sorption data in Table 3 can be described using eqs 4–6, as illustrated by the solid lines and curves in Figure 2a–f. To fit the data to this model, we obtain the saturation pressures for the penetrants, used to calculate f_{sat} , from the literature,²⁵ and the penetrant partial molar volumes in the polymer are the average values obtained in various polymer/gas systems by Kamiya and co-workers;³² these values are recorded in Table 1. The \bar{V}_2 values are taken to be independent of temperature. Additionally, the effect of temperature and penetrant fugacity on the polymer

sample volume was neglected, and this assumption is evaluated as follows. Typically, the sorbed penetrant swells the polymer sample, and, thus, increases the sample volume and decreases the volume of the gas phase in the sorption experiments. The maximum penetrant volume fraction (i.e., $\phi_{2,\text{max}}$, which is obtained at the lowest temperature and highest fugacity) is less than 0.010, except for C_2H_4 at -20°C (which is 0.03) and CO_2 at -20°C (which is 0.12). If such an effect is included in analyzing the sorption data, then the calculated sorption values are very close to the values reported in Table 3, and the difference is typically less

Table 3. Gas Concentration in XLPEGDA as a Function of Temperature and Fugacity^a

gas	308 K		298 K		273 K		263K		253K	
	<i>f</i>	<i>C</i>	<i>f</i>	<i>C</i>	<i>f</i>	<i>C</i>	<i>f</i>	<i>C</i>	<i>f</i>	<i>C</i>
CH ₄	3.6	0.47	3.6	0.46	3.7	0.62	3.6	0.52	3.7	0.51
	5.9	0.78	7.1	0.88	7.1	1.23	7.0	1.05	6.9	0.92
	7.2	0.91	10.3	1.28	10.4	1.81	10.2	1.50	10.3	1.31
	8.6	1.11	13.5	1.70	13.5	2.41	13.4	2.02	13.4	1.80
	10.4	1.31								
	14.0	1.85								
C ₂ H ₄	1.6	1.04	2.9	2.13	2.4	2.49	1.5	1.51	1.7	2.01
	3.2	2.13	5.3	3.97	4.8	5.16	3.7	4.18	3.9	4.93
	4.8	3.22	7.9	5.99	7.1	7.79	6.2	7.09	6.3	8.41
	6.5	4.35	10.2	7.81	9.2	10.2	8.9	10.6	8.9	13.1
	8.0	5.30								
	9.5	6.55								
	11.0	7.61								
	12.5	8.78								
C ₂ H ₆	1.7	0.83	2.9	1.58	1.6	1.20	2.6	1.98	3.0	2.43
	3.3	1.69	5.6	3.11	3.5	2.55	8.7	7.28	5.9	5.14
	4.9	2.49	8.4	4.71	5.6	4.35				
	6.5	3.32	11.0	6.26	8.2	6.48				
	8.1	4.16								
	9.5	4.93								
	10.9	5.64								
	12.3	6.44								
CO ₂	1.3	1.8	1.3	2.2	1.1	3.6	0.93	4.0	0.83	4.6
	2.8	3.9	3.4	5.9	2.2	7.3	2.4	10.7	1.6	9.3
	4.4	6.1	5.1	8.9	3.6	12.0	3.9	17.7	2.2	12.6
	5.9	8.2	6.9	12.2	5.0	17.0	5.9	27.6	3.6	21.9
	7.4	10.5	9.2	16.5	6.5	22.5	8.3	40.7	3.8	23.9
	8.9	12.7			8.1	28.8	10.1	51.2	5.3	34.3
	10.0	14.4			10.0	36.6			7.3	49.4
	11.2	16.2							9.9	72.5
C ₃ H ₆	0.93	1.92	1.2	2.8	0.95	4.1	0.54	2.45		
	1.9	4.11	2.1	5.5	1.7	7.7	0.98	4.70		
	2.8	6.24	3.0	8.2	2.4	11.6				
	3.6	8.26	4.1	11.9						
	4.4	10.4	5.2	15.6						
	4.9	11.9								
C ₃ H ₈	1.4	1.65	1.1	1.6	0.98	2.03	0.84	1.88	0.61	1.46
	2.5	3.05	2.3	3.3	1.4	3.03	1.4	3.25	0.93	2.54
	3.6	4.64	3.3	5.0	1.9	4.15			1.2	3.62
	4.6	6.12	4.9	7.5	2.4	5.34				

^a Note: *f* is expressed in atm and *C* is expressed in cm³(STP)/cm³ polymer.

than 10% (which is a typical uncertainty value for gas solubility, cf. Table 8), even for CO₂ at $\phi_{2,\max}$. Furthermore, this swelling effect could be offset partially by the decrease in the polymer sample volume as temperature decreases. For example, the thermal expansion coefficient of XLPEGDA was estimated to be $8.4 \times 10^{-4} \text{ K}^{-1}$ ¹³ and, thus, as temperature decreases from 25 °C to −20 °C, sample volume decreases by about 4%. Therefore, to simplify the analysis, these effects are neglected, that is, the polymer sample density is assumed to be constant in the temperature range studied, and the swelling effect on sorption results is neglected.

The detailed values of χ_0 , χ_1 , and χ_2 are recorded in Table 4. The uncertainty in these parameters was estimated by a standard propagation of error analysis.³³ Because the CH₄ isotherms are essentially linear, the solubility and Flory–Huggins χ parameter of CH₄ do not depend on the penetrant volume fraction. Figure 4 presents the effect of temperature and penetrant volume fraction on χ in XLPEGDA. The points are experimental data calculated using eqs 4–5, and the lines are based on eq 6 using the adjustable parameters χ_0 , χ_1 , and χ_2 .

In general, the empirical equation, eq 6, describes the data satisfactorily, and χ is a weak function of the penetrant volume fraction in the polymer, ϕ_2 .

($\chi_0 + \chi_2$) has been added to the original Flory–Huggins model in an empirical fashion to account for the concentration dependence of χ and to account for noncombinatorial contributions to the entropy of mixing; the value of ($\chi_0 + \chi_2$) in the original theory is 0.³⁴ For C₂H₄, C₂H₆, and C₃H₆ in XLPEGDA, ($\chi_0 + \chi_2$) values are near zero (cf., Table 4). However, this is not true for CH₄, CO₂, and C₃H₈ in XLPEGDA. For example, CH₄ has a value of −3.8 for ($\chi_0 + \chi_2$). For all penetrants except CO₂, χ_1 values are positive, so increasing temperature decreases χ . This trend has been observed in many systems, such as CO₂ sorption in 1,2-polybutadiene, poly(ethylene-co-vinyl acetate) and PDMS,³² and methoxyflurane sorption in PDMS.³⁵ However, for CO₂ in XLPEGDA, χ_1 is negative and, therefore, the χ value decreases as temperature decreases, which suggests that the interaction between CO₂ and XLPEGDA becomes stronger and more favorable at lower temperatures.

Historically, χ_1 has been related to solubility parameters as follows³⁶

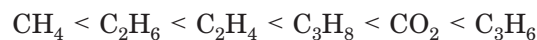
$$\chi_1 = \frac{\bar{V}_2}{R}(\delta_1 - \delta_2)^2 \quad (7)$$

where δ_1 and δ_2 are the solubility parameters of XLPEGDA and the penetrant of interest, respectively. Because XLPEGDA contains 82% PEO, δ_1 is presumed to be similar to that of pure PEO, that is, 19.8 MPa^{0.5}.¹⁹ Because the value of ($\chi_0 + \chi_2$) in the original theory is 0, χ_1 in eq 7 is often replaced by χT in the literature.^{37,38} Using this approach and 19.8 MPa^{0.5} for the solubility parameter of XLPEGDA, we estimated the solubility parameters of the penetrants at 25 °C. The resulting solubility parameters (i.e., $\delta_{2,\text{exp}}$) are listed in Table 4.²⁵ The literature values of penetrant solubility parameters, $\delta_{2,\text{lit}}$, are also included in the table for comparison; these values are calculated from gas solubility in liquids, where χ_1 is assumed to be equal to χT .³⁷ Except for CO₂, $\delta_{2,\text{exp}}$ values are near but slightly lower than $\delta_{2,\text{lit}}$. This agreement is considered satisfactory given the assumptions involved in making this comparison.

Solubility Correlations. Infinite dilution solubility coefficients, S_A^∞ , were estimated using eqs 3–6 in the limit as gas fugacity approaches zero

$$S_A^\infty = \lim_{f \rightarrow 0} \frac{C}{f} = \frac{22\,414}{f_{\text{sat}} \bar{V}_2} \exp(-1 - \chi^\infty) \quad (8)$$

where χ^∞ is the Flory–Huggins interaction parameter, χ , at infinite dilution and at the temperature of interest. Figure 5 presents penetrant infinite dilution solubility at various temperatures. S_A^∞ increases in the following order at most of the temperatures considered:



Olefins (e.g., C₂H₄ and C₃H₆) are more soluble than their paraffin analogues, even though olefins have lower critical temperatures (as shown in Table 1) and are, therefore, less condensable (and, in turn, often less soluble in polymers) than the corresponding paraffins.³⁹ The higher sorption of olefins probably derives from favorable interactions between the double bonds in the

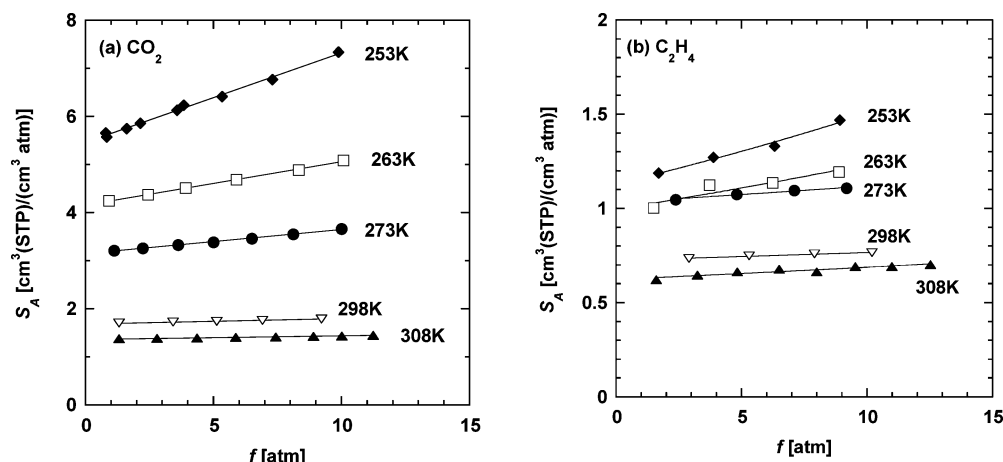


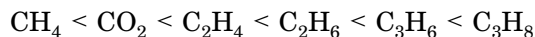
Figure 3. Effect of penetrant fugacity (f) and temperature on gas solubility in XLPEGDA. (a) CO_2 ; (b) C_2H_4 .

Table 4. Fitting Constants Used to Describe Experimental Solubility Data^a

penetrant	χ_0	χ_1 (K)	χ_2	$\chi_0 + \chi_2$	$\delta_{2\text{exp}}^{\circ}$ (MPa ^{0.5})	$\delta_{2\text{lit}}^{\circ}$ (MPa ^{0.5})
CH_4	-3.8 ± 0.2	1590 ± 50	0	-3.8	10.7 ± 0.5	11.6
C_2H_4	-0.33 ± 0.10	485 ± 25	0.24 ± 0.1	-0.09	11.6 ± 0.2	12.4
C_2H_6	1.5 ± 0.1	750 ± 30	-1.9 ± 0.1	-0.4	10.4 ± 0.2	12.4
CO_2	3.7 ± 0.2	-360 ± 30	-1.6 ± 0.1	2.1	26.8 ± 0.5	21.8 ¹³
C_3H_6	-0.86 ± 0.10	490 ± 30	0.84 ± 0.10	-0.02	12.4 ± 0.3	13.2
C_3H_8	-0.89 ± 0.1	980 ± 30	-0.13 ± 0.1	-1.0	11.4 ± 0.2	13.1

^a Note: The solubility parameter of XLPEGDA is $19.8 \text{ MPa}^{0.5}$.¹⁹ $\delta_{2\text{exp}}$ is the value of penetrant solubility parameter estimated from eq 7 using the χ value at infinite dilution, instead of χ_1 . $\delta_{2\text{lit}}$ is the value of the penetrant solubility parameter at 25 °C from the DIPPR database.²⁵

olefins and the polar ether oxygen in the polymer; a similar phenomenon is observed in poly(ethylene oxide).¹⁹ On the basis of their similar critical temperatures, CO_2 and C_2H_6 have essentially the same condensability. In nonpolar rubbery polymers such as polyethylene (PE)³⁹ and poly(dimethylsiloxane) (PDMS),⁴⁰ C_2H_6 has higher solubility than CO_2 . However, polar XLPEGDA exhibits much higher CO_2 solubility than C_2H_6 solubility, which is ascribed to specific interactions between quadrupolar CO_2 and polar ether oxygens in XLPEGDA. In general, the increasing order of penetrant solubility in XLPEGDA is quite different from that observed in nonpolar polymers, such as PE³⁹ and PDMS,⁴⁰ where gas solubility often increases systematically with increasing condensability (as characterized by T_c). For example, gas solubility in low-density PE increases in the following order:⁴¹



Because of the lack of specific interactions between PE and these penetrants, solubility selectivity is dominated mainly by relative penetrant condensability.

It is customary to relate S_A^∞ to penetrant condensability,⁴² which could be characterized by critical temperature, T_c (K). The following equation has been used widely^{42–44}

$$\ln S_A^\infty = a' + b'T_c \quad (9)$$

where a' and b' are constants depending on the polymer and the temperature. Figure 6 presents a fit of eq 9 to gas solubility data at 298 and 263 K. Clearly, the model does not describe the experimental data well, especially for CO_2 and C_3H_6 . Equation 9 assumes that gas solubil-

ity is determined only by its condensability (as characterized by T_c), so the effect of interactions between the polymer and a specific gas on solubility is neglected. However, this is not the case in polar XLPEGDA. Additionally, eq 9 does not allow gas solubility to vary with temperature, and this feature is clearly not consistent with the experimental data. For this reason, a different set of a' and b' values are required for each temperature considered. Gee developed an expression relating $\ln S_A^\infty$ to penetrant normal boiling point (i.e., T_b) using rather straightforward thermodynamic arguments.⁴⁵ Empirically, T_b can be related to T_c by the Guldberg–Guye rule:⁴⁶ $T_b = 0.6T_c$. Using this approach, Barrer and Skirrow obtained⁴⁶

$$\ln S_A^\infty = -(a + \chi^\infty) + bT_c \quad (10)$$

where $a = 4.5$ and $b = 6/T$, in the original theory when solubility has units of $\text{cm}^3(\text{STP})/(\text{cm}^3 \text{ atm})$. Often in the literature, $(a + \chi^\infty)$ and b are treated as adjustable parameters to fit eq 10 to experimental data. The value of b varies from 0.016 to 0.019 K^{-1} at 25 °C or 35 °C for polymer/penetrant systems without specific interactions.³⁰ In our case, to account for the differences in χ^∞ parameters among different penetrants, we present the values of $(\ln S_A^\infty + \chi^\infty)$ as a function of T_c at various temperatures in Figure 7. The lines in the figure are drawn on the basis of eq 10. The values of a and b are recorded in Table 5, and they are roughly similar to the theoretical values. However, the temperature dependence of a and b are not captured by this simple model (i.e., eq 10). Qualitatively, the trend in infinite dilution solubility is well described by eq 10 at each temperature. The success in describing the data using eq 10, compared to eq 9, is due to inclusion of the Flory–Huggins

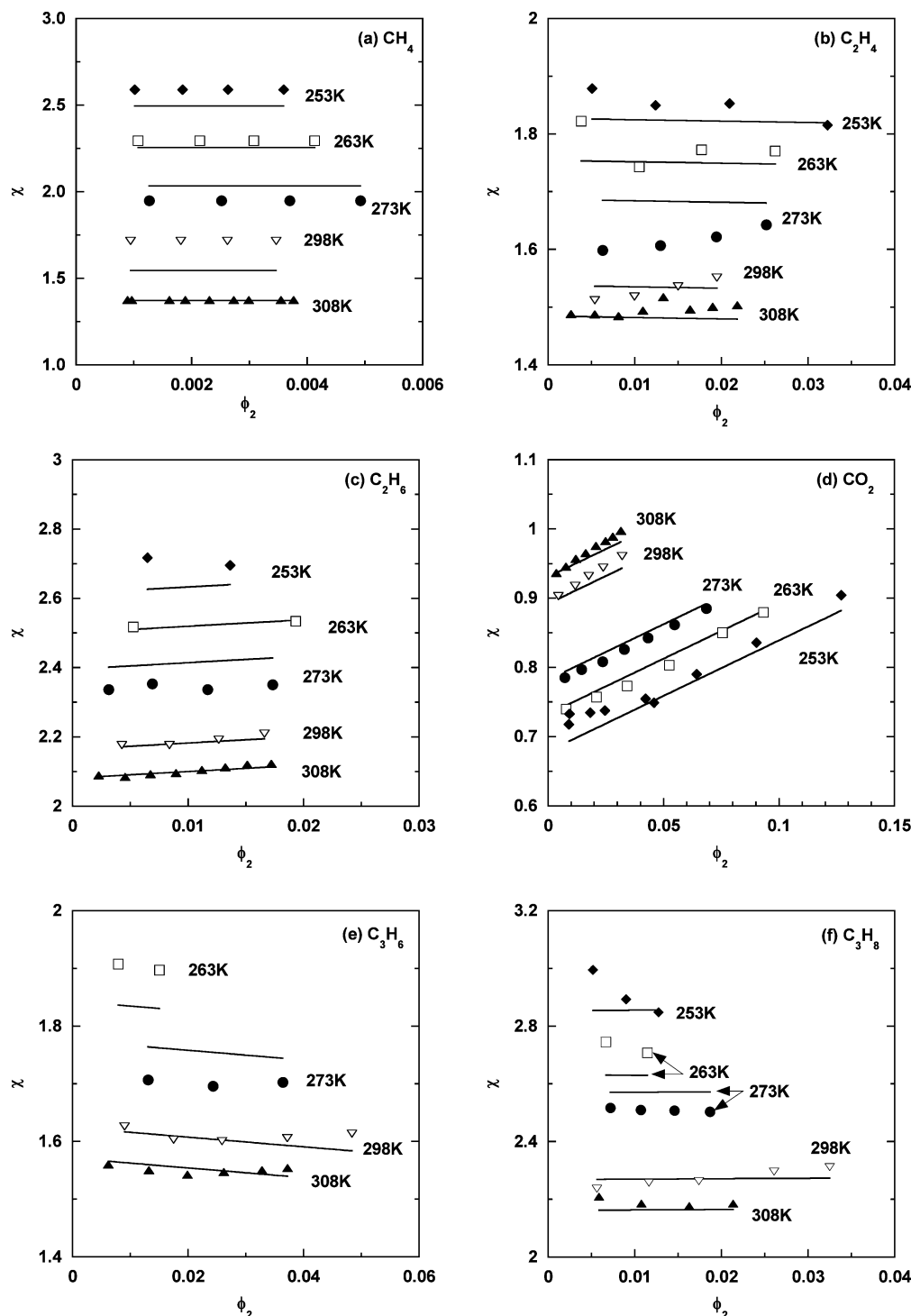


Figure 4. Effect of temperature and penetrant volume fraction, ϕ_2 , on polymer/penetrant interaction parameters, χ , in XLPEGDA. $T = 308$ K (▲), 298 K (▽), 273 K (●), 263 K (□), and 253 K (◆). The points are calculated using eqs 4–5, and the lines are based on eq 6 using the adjustable parameters, χ_0 , χ_1 , and χ_2 , which are recorded in Table 4.

interaction parameter in eq 10, which accounts for the effect of polymer/gas interactions on solubility. In contrast, eq 9 assumes either a negligible effect of interactions on gas solubility or equivalent interactions between the polymer and various penetrants. This assumption may be valid in some cases.⁴⁰ However, for polar polymers such as XLPEGDA, these interactions contribute significantly to the sorption and, therefore, cannot be ignored.

It is of interest to examine other correlations between solubility and penetrant condensability. Stern reported

the following empirical equation²⁴

$$\ln S_A^\infty = M + N \left(\frac{T_c}{T} \right)^2 \quad (11)$$

where M and N are adjustable constants. Bondar et al. derived an expression similar to eq 11.⁴⁷ Unlike eq 9 or 10, this relation accounts explicitly for the effect of temperature on solubility and, thus, it offers the possibility of describing all of the XLPEGDA sorption data using only one set of adjustable constants (e.g., M and

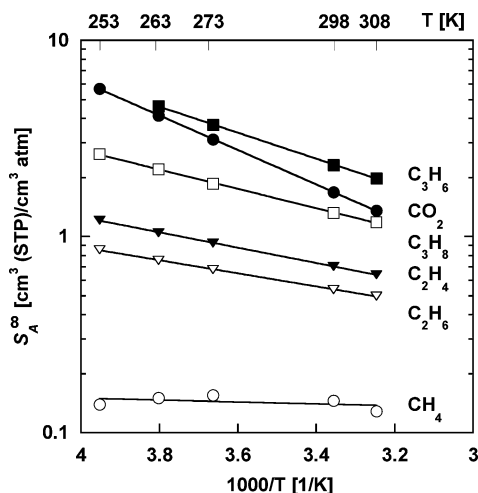


Figure 5. Infinite dilution solubility of various penetrants as a function of temperature in XLPEGDA.

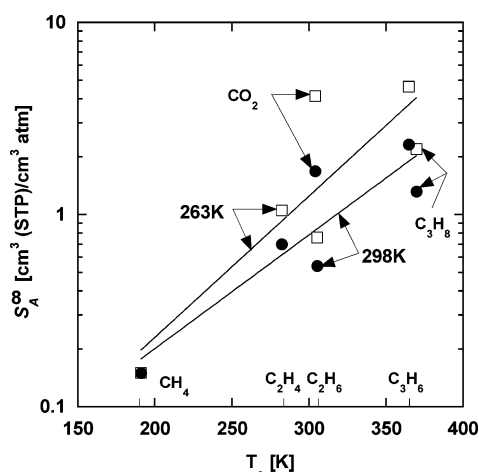


Figure 6. Infinite dilution solubility of various penetrants in XLPEGDA as a function of penetrant condensability, as represented by the penetrant critical temperature (T_c).

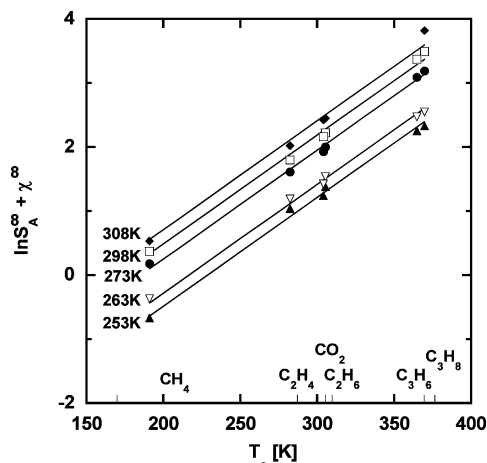


Figure 7. The values of $(\ln S_A^\infty + \chi^\infty)$ as a function of T_c at 308 K (◆), 298 K (□), 273 K (●), 263 K (▽), and 253 K (▲).

N), instead of 5 different sets of parameter values. This empirical equation has been used successfully to describe the solubility of a wide range of noninteracting penetrants in rubbery polymers such as polyethylene,²⁴ polyisobutylene,⁴⁸ PDMS,^{35,40} polystyrene^{49,50} and glassy polymers such as poly(5,6-bis(trimethylsilyl)norborene)⁵¹ and poly(2,2-bis(trifluoromethyl)-4,5-difluoro-1,3-diox-

Table 5. Model Parameters Describing Solubility as a Function of Temperature and Penetrant Critical Temperature^a

T (K)	a_{theory}	a_{exp}	$b_{\text{theory}} = 6/T$	b_{exp}
308	4.5	3.9 ± 0.4	0.019	0.017 ± 0.001
298	4.5	3.7 ± 0.4	0.020	0.017 ± 0.001
273	4.5	3.2 ± 0.4	0.022	0.017 ± 0.001
263	4.5	2.9 ± 0.4	0.023	0.017 ± 0.001
253	4.5	2.7 ± 0.4	0.024	0.017 ± 0.001

^a Note: a_{exp} and b_{exp} values are obtained by fitting eq 10 to estimates of S_A^∞ from eq 8.

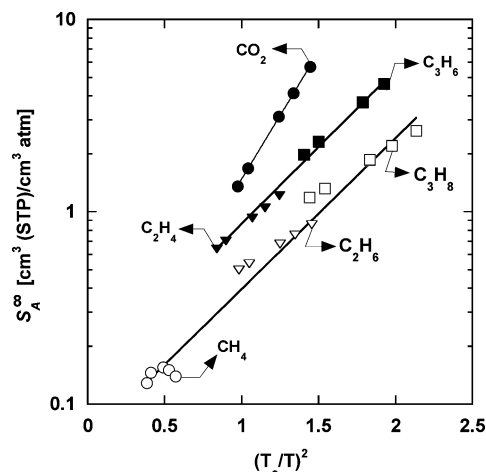


Figure 8. Penetrant infinite dilution solubility in XLPEGDA as a function of $(T_c/T)^2$.

ole-co-tetrafluoroethylene) (AF2400⁵² and AF1600⁵³). Figure 8 presents S_A^∞ as a function of $(T_c/T)^2$. Three trendlines are observed: one for normal paraffins (e.g., CH_4 , C_2H_6 , and C_3H_8) that do not interact specifically with the polymer; one for olefins (e.g., C_2H_4 and C_3H_6) that interact somewhat favorably with the polymer; and the last one for CO_2 , which interacts strongly and favorably with XLPEGDA. The fitting parameters (i.e., M and N) are presented in Table 6 for these three different lines, and they are compared to those in other polymers. The satisfactory modeling of paraffins is consistent with results obtained using this relation to describe sorption in nonpolar polymers such as PE and PDMS.³⁵ For paraffins, differences in the critical temperatures among the penetrants provide the dominant contribution to their solubility in XLPEGDA. The positive deviation of olefins and CO_2 solubility from the paraffin line could be ascribed to favorable interactions between the polymer and these gases. The more positive deviation of CO_2 solubility is consistent with more favorable interactions between CO_2 and the polymer, which is also manifested in lower χ values. These phenomena have also been observed for other polar polymers.^{54,55} Tseng et al. reviewed gas solubility in polar poly(vinyl acetate) and reported different fitting parameters for different categories of penetrants, such as polar and nonpolar penetrants, as shown in Table 6.⁵⁴ Interestingly, the N value for CO_2 in XLPEGDA is quite close to the value for the sorption of polar penetrants in poly(vinyl acetate). Sanchez and Rogers estimated gas solubility coefficients in three nonpolar or weakly polar polymers (i.e., polystyrene, poly(1-butene) and atactic-polypropylene) and two polar polymers (i.e., poly(vinyl acetate) and poly(methyl acrylate)) using a lattice fluid model and the geometric mean approximation for interactions between the polymer

Table 6. Comparison of Adjustable Parameters in the Correlation between $\ln S_A^\infty$ and $(T/T_c)^2$

polymer		penetrant	N	M	ref
glassy	AF1600	hydrocarbons	2.19	-0.99	53
	AF2400	all	2.56	-0.81	52
	polyethylene	all	2.63	-2.97	24
	PDMS	all	2.48	-1.70	35
	polystyrene	fluoro/hydrocarbons	2.71	-2.35	50
rubbery	poly(vinyl acetate)	nonpolar; nonaromatic	2.17	-2.49	54
		aromatic	2.20	-1.58	
		polar	2.69	-2.01	
	XLPEGDA	CH ₄ , C ₂ H ₆ , C ₃ H ₈	1.8 ± 0.1	-2.8 ± 0.1	this study
		C ₂ H ₄ , C ₃ H ₆	1.9 ± 0.1	-2.1 ± 0.1	
		CO ₂	3.0 ± 0.1	-2.6 ± 0.1	

Table 7. Enthalpies of Sorption, Condensation, and Mixing for Gas Sorption in Rubbery XLPEGDA, Polyethylene (GreX),³⁹ and Glassy AF2400⁵² at Infinite Dilution^a

polymer		CH ₄	CO ₂	C ₂ H ₄	C ₂ H ₆	C ₃ H ₆	C ₃ H ₈
PE	ΔH_S	-2.9	-5.4		-9.6	-13.0	-12.6
AF2400	ΔH_S	-13.2	-14.8		-14.2		-20.9
XLPEGDA	S_{A0}	95 ± 15	1.8 ± 0.1	34 ± 4	41 ± 3	14 ± 2	29 ± 4
	ΔH_S	-1 ± 2	-17 ± 1	-7.5 ± 1.4	-6.4 ± 1.4	-13 ± 2	-9.4 ± 1.4
	ΔH_{cond}		-10.2	-5.4	-9.1	-15.8	-16.5
	ΔH_{mix}		-6.8 ± 1	-2.1 ± 1.4	2.7 ± 1.4	2.8 ± 2	7.1 ± 1.4

^a Note: S_{A0} has units of $10^{-3} \text{ cm}^3/(\text{cm}^3 \text{ atm})$ and enthalpies are reported in kJ/mol. ΔH_{cond} is evaluated at 273 K.

segments and gases.⁵⁵ In general, excellent agreement between the estimated and experimental solubility was observed for gas sorption in the three nonpolar polymers, although the solubility of oxygen-containing penetrants (ethers, esters, and ketones) were overestimated. For the two polar polymers, the solubility coefficients of the nonaromatic hydrocarbons were overestimated systematically, whereas solubility coefficients of polar and aromatic penetrants were well correlated.⁵⁵ They claimed that the deviations were caused by interactions between polymers and penetrants that were not accounted for by the geometric mean approximation.⁵⁵

Enthalpy of Sorption. In general, S_A^∞ increases with decreasing temperature, as illustrated in Figure 5, and the temperature dependence is usually described as follows⁴²

$$S_A^\infty = S_{A0} \exp\left(-\frac{\Delta H_S}{RT}\right) \quad (12)$$

where S_{A0} is a preexponential factor, and ΔH_S is the enthalpy of sorption. The lines in Figure 5 are best fits of the data to eq 12. The values of S_{A0} and ΔH_S are recorded in Table 7. Based on the two hypothetical thermodynamic steps for gas sorption discussed before, ΔH_S is given by³⁸

$$\Delta H_S = \Delta H_{\text{cond}} + \Delta H_{\text{mix}} \quad (13)$$

where ΔH_{cond} is the enthalpy change due to gas condensation and ΔH_{mix} is the enthalpy change in the mixing step. Equation 13 is often used qualitatively to explain ΔH_S differences for various penetrants. ΔH_{cond} depends on temperature for a given penetrant. We use ΔH_{cond} values at 273 K (i.e., the median of the temperature range explored in this study) to qualitatively understand the changes in ΔH_{mix} from one penetrant to another.⁵⁶ The results are recorded in Table 7. Values of ΔH_S for all of the penetrants are negative since solubility increases as temperature decreases. ΔH_{mix} values for CO₂ and C₂H₄ in XLPEGDA are negative,

which is not expected on the basis of the Flory–Huggins model or regular solution theory.³⁷ Nevertheless, negative ΔH_{mix} values for penetrant sorption in rubbery polymers have been reported. For example, in poly(dimethylsiloxane) (PDMS), ΔH_{mix} is -3 kJ/mol for propane,⁵⁶ -2.72 kJ/mol for trichloromethane,⁵⁷ and -3.97 kJ/mol for trichloroethylene.⁵⁷ A detailed, molecular level explanation of negative ΔH_{mix} values is beyond the scope of the simple model (e.g., the Flory–Huggins model) often used to interpret such measurements. In this study, the slightly negative ΔH_{mix} value for C₂H₄ sorption in XLPEGDA is consistent with weak, favorable interactions between olefins and polar ether oxygens, and the more negative value of ΔH_{mix} for CO₂ can be interpreted as another sign of significant favorable interactions between CO₂ and the polymer.

Favorable interactions lead to lower ΔH_{mix} and, therefore, lower ΔH_S . Olefins such as C₂H₄ and C₃H₆ have lower ΔH_{mix} values than their paraffin analogues, and CO₂ has the lowest ΔH_{mix} value among all of the penetrants studied. Except for CO₂, which strongly interacts with the polymer and has a very low ΔH_{mix} value, ΔH_S is dominated by ΔH_{cond} , and, therefore, ΔH_S decreases with increasing T_c .

Table 7 also compares the ΔH_S values in XLPEGDA with those in nonpolar PE (GreX with a crystallinity of 69–78 vol %)³⁹ and glassy AF2400.⁵² All of the penetrants exhibit less negative values of ΔH_S in polar XLPEGDA than those in the other two polymers, except for CO₂. Because penetrant condensability is independent of the polymer, this difference must be ascribed to differences in ΔH_{mix} . In general, paraffins have less favorable interactions with polar polymers than with nonpolar polymers such as PE, resulting in more positive values of ΔH_{mix} for these gases in polar polymers. These differences decrease for olefins, probably because of the affinity between the double bonds in the olefins and the polar groups in XLPEGDA. The ΔH_S value of CO₂ is more negative in XLPEGDA than in the other polymers because of the favorable interactions between polar XLPEGDA and CO₂. Glassy polymers such as AF2400 have nonequilibrium excess volume (or Lang-

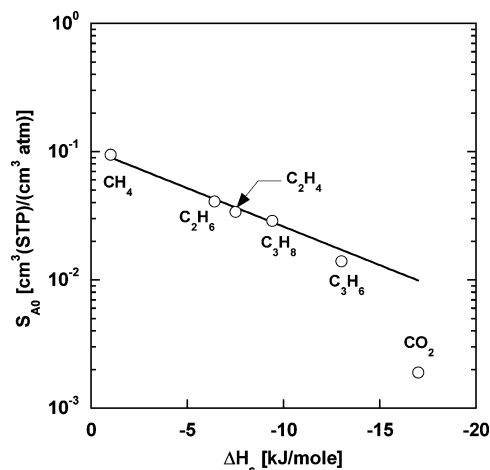


Figure 9. Correlation of the pre-exponential factor, S_{A0} , with ΔH_S in XLPEGDA. The line is drawn based on eq 14 using literature values of μ and v .⁴²

muir sorption sites) that significantly decreases ΔH_S .⁵² However, because of the lack of specific interactions with CO_2 , the ΔH_S value of CO_2 is still higher in AF2400 than in XLPEGDA.

Figure 9 presents a correlation between the solubility preexponential factor, S_{A0} , and ΔH_S . The following empirical relation is often observed between these two parameters⁴⁷

$$\ln S_{A0} = \mu + v\Delta H_S \quad (14)$$

where μ and v are -2.27 and 0.138 when S_{A0} has units of $\text{cm}^3(\text{STP})/(\text{cm}^3 \text{ atm})$ and ΔH_S has units of kJ/mol , for the sorption of nonpolar penetrants in rubbery polymers.⁴² As illustrated in Figure 9, the experimental data obey this correlation in XLPEGDA, with the exception of CO_2 . The S_{A0} value of CO_2 is much lower than the line shown in Figure 9. $\ln S_{A0}$ is proportional to the entropy change of solution.⁴⁷ Presumably, the favorable interactions between a polymer and a penetrant might lead to a certain degree of order when the penetrant is sorbed in the polymer.⁵⁸ This behavior has also been observed in liquid mixtures such as the chloroform/acetone system in which unlike molecules form hydrogen bonds but the like molecules cannot, and, therefore, there is a strong tendency to form chloroform–acetone pairs, which decreases the entropy of mixing.³⁸ In this case, CO_2 enjoys a strong and favorable interaction with XLPEGDA and, therefore, this interaction could decrease the CO_2 entropy in the polymer, the entropy change upon mixing and, thus, S_{A0} .

Solubility Selectivity. The effect of temperature on pure gas CO_2 /paraffin (i.e., CO_2/CH_4 and $\text{CO}_2/\text{C}_2\text{H}_6$) solubility selectivity in XLPEGDA is presented in Figure 10. The detailed values are also recorded in Table 8. Selectivity increases as temperature decreases, primarily because CO_2 solubility increases more with decreasing temperature than that of the other gases because of the favorable interactions between CO_2 and polar XLPEGDA. In particular, CO_2 and C_2H_6 have similar critical temperature (i.e., condensability). However, $\text{CO}_2/\text{C}_2\text{H}_6$ solubility selectivity increases from 2.7 to 6.6 as temperature decreases from 35°C to -20°C . CO_2/CH_4 solubility selectivity increases from 11 at 35°C to 41 at -20°C , which could potentially be useful for designing membrane materials for CO_2 removal from natural gas or other light gases. Figure 10 also presents olefin/

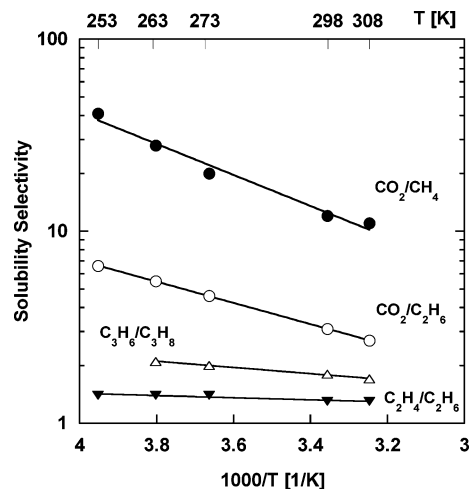


Figure 10. Effect of temperature on gas solubility selectivity at infinite dilution in XLPEGDA.

paraffin ($\text{C}_2\text{H}_4/\text{C}_2\text{H}_6$ and $\text{C}_3\text{H}_6/\text{C}_3\text{H}_8$) solubility selectivity as a function of temperature. These selectivities increase slightly with decreasing temperature, which is consistent with the slightly more negative ΔH_S values for olefins than the corresponding paraffins.

Table 9 compares CO_2 solubility and CO_2/CH_4 and $\text{CO}_2/\text{C}_2\text{H}_6$ solubility selectivity in XLPEGDA with those in rubbery polar cross-linked poly(propylene glycol) diacrylate (XLPPGDA), nonpolar PE³⁹ and PDMS,⁴⁰ nonpolar liquid hexane,^{13,59} and polar liquid tetrahydrofuran (THF).^{13,59,60} XLPEGDA exhibits higher CO_2 solubility and much higher CO_2/CH_4 and $\text{CO}_2/\text{C}_2\text{H}_6$ solubility selectivity than nonpolar PE and PDMS. Interestingly, XLPPGDA exhibits similar CO_2 solubility but lower CO_2/CH_4 solubility selectivity. XLPPGDA contains 86 wt % propylene oxide units and, therefore, can be regarded crudely as amorphous poly(propylene oxide). It has much higher fractional free volume (0.165 , which is calculated based on its density, $1.059 \pm 0.004 \text{ g/cm}^3$) than XLPEGDA, which increases gas solubility.¹³ Additionally, XLPPGDA has a lower content of ether oxygens than XLPEGDA, and they are probably less sterically accessible for interaction than those in XLPEGDA. Therefore, interactions with CO_2 in XLPPGDA would not be as favorable as in XLPEGDA, which could contribute to lower CO_2/CH_4 solubility selectivity. The effect of the decreased ether oxygen concentration (which would tend to make CO_2 less soluble in XLPPGDA than in XLPEGDA) appears to be offset by the effect of increased fractional free volume in XLPPGDA (which would tend to increase the solubility of all gases). As a result, CO_2 solubility remains similar in these two polymers, but CO_2/CH_4 solubility selectivity is lower in XLPPGDA than in XLPEGDA. Liquids usually exhibit higher gas solubility than the corresponding polymers with similar chemistry.¹³ Because of the lack of specific interactions with CO_2 , nonpolar hexane exhibits much lower solubility selectivity than XLPEGDA. Polar THF, which has one ether linkage for every four $-\text{CH}_2-$ linkages, has higher CO_2 solubility than XLPEGDA. However, THF has lower CO_2/CH_4 and $\text{CO}_2/\text{C}_2\text{H}_6$ solubility selectivity than XLPEGDA, presumably because of the lower concentration of ether oxygens in THF than in XLPEGDA.

Figure 11a–b presents the effect of fugacity on pure gas CO_2/CH_4 and $\text{CO}_2/\text{C}_2\text{H}_6$ solubility selectivities in XLPEGDA at 35°C and -20°C . The points are

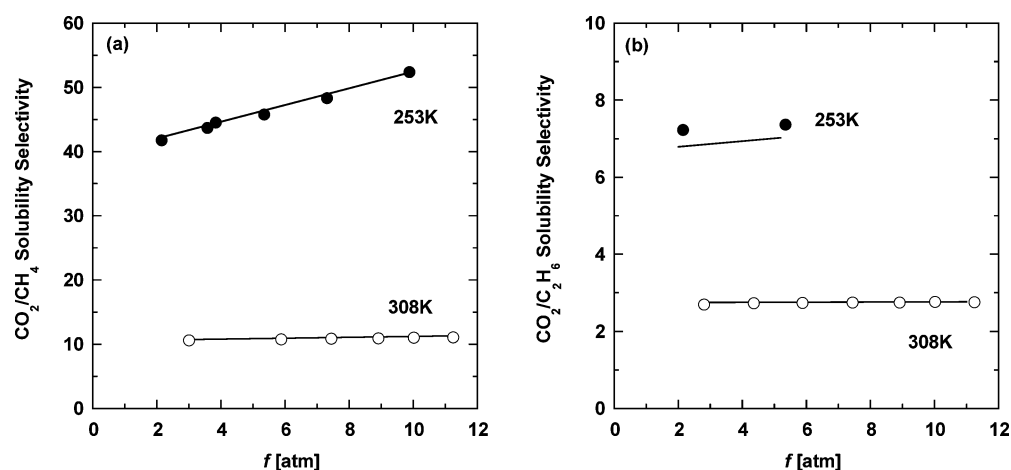
Table 8. Effect of Temperature on Infinite Dilution Solubility and Solubility Selectivity in XLPEGDA

<i>T</i> (K)	solubility (cm ³ (STP)/(cm ³ atm))			solubility selectivity			
	CO ₂	C ₂ H ₄	C ₃ H ₆	CO ₂ /CH ₄	CO ₂ /C ₂ H ₆	C ₂ H ₄ /C ₂ H ₆	C ₃ H ₆ /C ₃ H ₈
308	1.4 ± 0.1	0.64 ± 0.05	2.0 ± 0.2	11	2.7	1.3	1.7
298	1.7 ± 0.2	0.70 ± 0.07	2.3 ± 0.2	12	3.1	1.3	1.8
273	3.1 ± 0.3	0.93 ± 0.10	3.7 ± 0.4	20	4.6	1.4	2.0
263	4.1 ± 0.4	1.0 ± 0.1	4.6 ± 0.4	28	5.5	1.4	2.1
253	5.7 ± 0.6	1.2 ± 0.1		41	6.6	1.4	

Table 9. Comparison of CO₂ and CH₄ Solubility and Solubility Selectivity in XLPEGDA, XLPPGDA, Polyethylene (PE), Poly(dimethylsiloxane) (PDMS), Hexane (at 1 atm), and Tetrahydrofuran (THF at 1 atm)^a

	XLPEGDA	XLPEGDA	XLPPGDA	PE ³⁹	PDMS ⁴⁰	Hexane ^{13,59}	THF ^{13,59,60}
<i>T</i> (°C)	25	35	35	25	25	25	25
<i>S</i> _{CO₂}	1.7	1.4	1.3	0.45	1.29	2.06	6.22
<i>S</i> _{CO₂} / <i>S</i> _{CH₄}	12	11	6.2	2.2	3.1	2.4	10
<i>S</i> _{CO₂} / <i>S</i> _{C₂H₆}	3.1	2.7		0.35	0.59	0.36	1.6

^a Note: Gas solubility coefficients have units of cm³(STP)/(cm³ atm). Gas solubility coefficients in polyethylene have been adjusted to amorphous phase values using eq 15.³⁹ All properties are at infinite dilution, unless otherwise indicated.

**Figure 11.** Effect of fugacity on (a) pure gas CO₂/CH₄ solubility selectivity and (b) pure gas CO₂/C₂H₆ solubility selectivity in XLPEGDA at 35 °C and -20 °C. The points are calculated using experimental data, from Table 3. The lines are drawn using eqs 3–6.

calculated on the basis of the experimental data, which are recorded in Table 3. The lines are drawn using eqs 3–6 and the fitting parameters χ_0 , χ_1 , and χ_2 . These selectivities are essentially independent of fugacity at 35 °C and increase with increasing fugacity at -20 °C. For example, as fugacity increases from 2 to 10 atm at -20 °C, CO₂/CH₄ selectivity increases by 25%, from 42 to 53, and CO₂/C₂H₆ increases by 10%, from 6.8 to 7.7. These increases are mainly due to the increase of CO₂ solubility with increasing fugacity, as shown in Figure 3.

Test of the Two-Phase Model. Previously, gas sorption has been measured in pure PEO, which contains 71 vol % crystallinity.¹⁹ In a rubbery polymer, the effect of crystallinity on penetrant sorption is often represented as follows^{39,61}

$$S_A = S_{A,a} \phi_a \quad (15)$$

where S_A is the observed solubility coefficient, $S_{A,a}$ is the solubility coefficient in the wholly amorphous polymer, and ϕ_a is the amorphous phase volume fraction in the semicrystalline polymer. This model (i.e., the two-phase model) was used to fit gas solubility data in a series of semicrystalline polyethylene samples with crystallinity values ranging from 41 to 78 vol %.³⁹ However, when gas solubility values were extrapolated to the wholly amorphous phase, the resulting solubility

values were often not consistent with those measured in a completely amorphous polymer of similar chemical structure. For example, Michaels and Bixler estimated a value of 3.97 cm³(STP)/(cm³ atm) for C₃H₈ solubility in wholly amorphous polyethylene at 25 °C. They did not have access to wholly amorphous polyethylene, so they compared this extrapolated value to the C₃H₈ solubility in natural rubber, which is 6.2 cm³(STP)/(cm³ atm) at 25 °C.³⁹ In general, natural rubber is chemically similar to polyethylene, so Michaels and Bixler argued that these two polymers should exhibit similar solubility, especially for noninteracting penetrants such as C₃H₈. However, it is not clear that natural rubber is a very good analogue for amorphous polyethylene, so this result should be interpreted with caution. Mogri and Paul measured CO₂ and CH₄ solubility in poly(alkyl acrylates) at temperatures above and below their melting temperatures, T_m .⁶² They obtained the wholly amorphous phase solubility (e.g., $S_{A,a}$) at T_m by extrapolating solubility from temperatures well above T_m to T_m using eq 12. The solubility in the semicrystalline phase (e.g., S_A) at T_m was obtained by extrapolating data from temperatures well below T_m to T_m . The amorphous phase volume fraction (e.g., ϕ_a) was calculated as the ratio of S_A to $S_{A,a}$, and the value obtained was about 0.30. However, the value of ϕ_a estimated from differential scanning calorimetry was 0.60. Discrepancies

Table 10. Gas Infinite Dilution Solubility, S_A^∞ , and Solubility Selectivity in Semicrystalline Poly(ethylene oxide) (S-C PEO), Amorphous PEO (Am-PEO) and Cross-Linked PEO (XLPEGDA) at 35 °C^a

gas	S_A^∞			$S_{CO_2}^\infty/S_A^\infty$	
	S-C PEO ¹⁹	Am-PEO ¹⁹	XLPEGDA	Am-PEO ¹⁹	XLPEGDA
CH ₄	0.078 ± 0.037	0.28 ± 0.14	0.13 ± 0.02	5 ± 3	11 ± 2
C ₂ H ₄	0.17 ± 0.02	0.62 ± 0.07	0.64 ± 0.05	2.1 ± 0.3	2.2 ± 0.2
C ₂ H ₆	0.12 ± 0.02	0.41 ± 0.04	0.50 ± 0.05	3.2 ± 0.4	2.8 ± 0.4
CO ₂	0.37 ± 0.02	1.3 ± 0.1	1.4 ± 0.1	1	1
C ₃ H ₆	0.58 ± 0.02	2.2 ± 0.1	2.0 ± 0.2	0.59 ± 0.05	0.7 ± 0.1
C ₃ H ₈	0.34 ± 0.01	1.3 ± 0.1	1.2 ± 0.1	1.0 ± 0.1	1.2 ± 0.1

^a Note: Solubility values have units of cm³(STP)/(cm³ atm).

between experimental results and the model prediction based on eq 15 have also been reported in other semicrystalline polymers, such as rubbery 1,4-polybutadiene.⁶³ The failure of eq 15 to describe such data has led to the conclusion that the interphase between an amorphous phase and a crystal phase might sorb gas.⁶⁴ Some polymer crystals, such as those in poly(4-methyl-1-pentene) (PMP), are less dense than their amorphous phase, and they are able to sorb gas.⁶⁵ Nevertheless, the two-phase model has been validated by other researchers in polymers such as polyethylene^{66–68} and copolyesters.⁶⁹ Therefore, the crystal morphology and processing conditions probably have a significant effect on gas solubility in semicrystalline polymers.

On the basis of conflicting reports in prior work as described above, it is interesting to explore the applicability of the two-phase model to PEO. XLPEGDA contains 82 wt % PEO, and thus could be roughly regarded as a model of amorphous PEO. Table 10 compares the solubility values of a variety of gases and solubility selectivity of CO₂ over the other penetrants in XLPEGDA, semicrystalline PEO at 35 °C, and the estimated amorphous phase solubility in PEO, which was calculated using eq 15 from solubility coefficients measured in semicrystalline PEO.¹⁹ The CH₄ solubility values in XLPEGDA and amorphous PEO differ slightly because of the low gas sorption in semicrystalline PEO (which has 71 vol % crystallinity) and the high uncertainty associated with measuring the CH₄ sorption in semicrystalline PEO.¹⁹ The excellent agreement between the solubility values in XLPEGDA and those in wholly amorphous PEO suggests that the two-phase model for solubility is valid for this system and that the sorption properties of XLPEGDA are dominated by the ethylene oxide units in the materials.

Conclusions

Sorption isotherms of CO₂ and hydrocarbons (i.e., CH₄, C₂H₄, C₂H₆, C₃H₆, and C₃H₈) in polar XLPEGDA are described satisfactorily using the Flory–Huggins model with χ parameter values that depend on the temperature and weakly on penetrant volume fraction. For all penetrants except CO₂, as temperature decreases, χ values increase, indicating more unfavorable interactions between penetrants and XLPEGDA at lower temperatures. In contrast, χ values for CO₂ in XLPEGDA decrease with decreasing temperature, indicating more favorable interactions between CO₂ and XLPEGDA. Linear correlations between $\ln S_A^\infty$ versus T_c or $(T/T_c)^2$, which often provide good models for gas sorption in nonpolar rubbery polymers, fail to correlate quantitatively the sorption of quadrupolar CO₂ and olefins in polar XLPEGDA. The following model, which

considers the effect of polymer/penetrant interactions on gas solubility, provides a satisfactory description of the data: $\ln S^\infty(\text{cm}^3(\text{STP})/(\text{cm}^3 \text{ atm})) + \chi^\infty = -a + 0.017T_c(K)$.

For highly sorbing penetrants such as CO₂ and C₃H₆, gas solubility increases as fugacity increases. Gas solubility increases with decreasing temperature, so ΔH_S values are negative. $|\Delta H_S|$ generally increases as penetrant critical temperature increases, and CO₂ exhibits the largest value of $|\Delta H_S|$, mainly because of negative values of ΔH_{mix} . Compared to nonpolar rubbery polymers such as polyethylene and glassy polymers such as AF2400, XLPEGDA generally exhibits lower $|\Delta H_S|$ values, except for CO₂.

Acknowledgment. We gratefully acknowledge partial support of this work by the Chemical Sciences, Geosciences and Biosciences Division, Office of Basic Energy Sciences, Office of Science, U.S. Department of Energy (Grant No. DE-FG03-02ER15362). This research work was also partially supported by the United States Department of Energy's National Energy Technology Laboratory under a subcontract from Research Triangle Institute through their Prime Contract No.: DE-AC26-99FT40675. This work was also prepared with the partial support of U.S. Department of Energy, under Award No. DE-FG26-01NT41280. However, any opinions, findings, conclusions, or recommendations expressed herein are those of the authors and do not necessarily reflect the views of the DOE.

Appendix

Pure gas fugacity can be calculated using the virial equation of state, which is given by^{38,70}

$$Z = \frac{pV}{RT} = 1 + B'p + C'p^2 + \dots \quad (\text{A1})$$

where Z is the compressibility factor, p is the pressure, V is the molar volume, R is the gas constant, T is the temperature of interest, and B' and C' are the second and third virial coefficients, respectively. The above expression, truncated after the $C'p^2$ term, is sufficient for describing the gas behavior in this study. The constants (i.e., B' and C'), which are functions of temperature, are available in the literature⁷¹ and are recorded in Table 11 for the penetrants and temperatures of interest to this study.

Pure gas fugacity (i.e., f) is related to gas pressure as follows^{38,70}

$$\ln \frac{f}{p} = \int_0^p \frac{Z - 1}{p} dp = B'p + \frac{1}{2} C'p^2 \quad (\text{A2})$$

Table 11. The Second and Third Virial Coefficients of Penetrants at Temperatures of Interest^{71 a}

gas	308 K		298 K		273 K		263 K		253 K	
	$B' \times 10^3$	$C' \times 10^6$	$B' \times 10^3$	$C' \times 10^6$	$B' \times 10^3$	$C' \times 10^6$	$B' \times 10^3$	$C' \times 10^6$	$B' \times 10^3$	$C' \times 10^6$
CH ₄	-1.58	1.49	-1.77	1.24	-2.40	-0.06	-2.74	-1.23	-3.08	-2.65
C ₂ H ₄	-5.21	-16.0	-5.74	-20.4	-7.49	-40.0	-8.28	-50.7	-9.44	-67.7
C ₂ H ₆	-6.88	-31.2	-7.64	-39.9	-9.88	-76.5	-11.0	-95.2	-12.3	-132
CO ₂	-4.54	-12.9	-5.05	-17	-6.74	-34.3	-7.38	-45.2	-8.24	-58.0
C ₃ H ₆	-12.8	-141	-14.2	-177	-18.4	-358	-20.1	-471		
C ₃ H ₈	-13.4	-293	-15.8	0	-21.0	0	-23.8	0	-26.2	0

^a Note: B' has units of atm⁻¹ and C' has units of atm⁻².

which can be written as follows:

$$f = p \exp\left(B'p + \frac{1}{2} C'p^2\right) \quad (\text{A3})$$

Equation A3 was used to calculate fugacity in this study. As shown in Table 11, the absolute values of B' and C' are very low, and thus in the pressure range considered in this study, the f/p values are a linear function of pressure, as shown in Figure 1, so eq A3 can be simplified as follows:

$$f = p(1 + B'p) \quad (\text{A4})$$

References and Notes

- (1) Baker, R. W. *Membrane Technology and Application*, 2nd ed.; J. Wiley: New York, 2004.
- (2) Kohl, A. L.; Nielson, R. *Gas Purification*, 5th ed.; Gulf Publishing: Houston, TX, 1997.
- (3) Petropoulos, J. H. In *Polymeric Gas Separation Membranes*; Paul, D. R., Yampolskii, Y. P., Eds.; CRC Press: Boca Raton, FL, 1994; pp 17–81.
- (4) Freeman, B. D.; Pinnau, I. In *Polymer Membranes for Gas and Vapor Separation*; Freeman, B. D., Pinnau, I., Eds.; ACS Symposium Series; Washington, DC, 1999; Vol. 733, pp 1–27.
- (5) Koros, W. J.; Coleman, M. R.; Walker, D. R. *B. Annu. Rev. Mater. Sci.* **1992**, *22*, 47–89.
- (6) Freeman, B. D.; Pinnau, I. *Trends Polym. Sci.* **1997**, *5*, 167–73.
- (7) Ghosal, K.; Chern, R. T.; Freeman, B. D.; Daly, W. H.; Negulescu, I. I. *Macromolecules* **1996**, *29*, 4360–9.
- (8) Stern, S. A. *J. Membr. Sci.* **1994**, *94*, 1–65.
- (9) Singh, A.; Freeman, B. D.; Pinnau, I. *J. Polym. Sci., Part B: Polym. Phys.* **1998**, *36*, 289–301.
- (10) *Today's Hydrogen Production Industry*; <http://www.fossil.energy.gov/programs/fuels/hydrogen/currenttechnology.shtml>.
- (11) Lin, H.; Freeman, B. D.; Toy, L. G.; Bondar, V. I.; Gupta, R. P.; Pas, S. J.; Hill, A. J. *J. Polym. Prepr. (Am. Chem. Soc., Div. Polym. Chem.)* **2004**, *45*, 23–4.
- (12) Baker, R. W.; Wijmans, J. G.; Kaschemekat, J. H. *J. Membr. Sci.* **1998**, *151*, 55–62.
- (13) Lin, H.; Freeman, B. D. *J. Mol. Struct.* **2005**, *739*, 57–74.
- (14) Blume, I.; Pinnau, I. U.S. Patent 4,963,165 1990.
- (15) Bondar, V. I.; Freeman, B. D.; Pinnau, I. *J. Polym. Sci., Part B: Polym. Phys.* **2000**, *38*, 2051–62.
- (16) Patel, N. P.; Miller, A. C.; Spontak, R. J. *Adv. Mater.* **2003**, *15*, 729–33.
- (17) Okamoto, K.-i.; Fujii, M.; Okamoto, S.; Suzuki, H.; Tanaka, K.; Kita, H. *Macromolecules* **1995**, *28*, 6950–6.
- (18) Hirayama, Y.; Kase, Y.; Tanihara, N.; Sumiyama, Y.; Kusuki, Y.; Haraya, K. *J. Membr. Sci.* **1999**, *160*, 87–99.
- (19) Lin, H.; Freeman, B. D. *J. Membr. Sci.* **2004**, *239*, 105–17.
- (20) Pinnau, I.; Freeman, B. D. *Polym. Mater. Sci. Eng.* **2002**, *86*, 108.
- (21) Merkel, T. C.; Toy, L. G.; Coker, D. T.; Gupta, R. P.; Freeman, B. D.; Fleming, G. K. *Proc. - Annu. Int. Pittsburgh Coal Conf.*, 19th, **2002**, 713–23.
- (22) Lin, H.; Kai, T.; Freeman, B. D.; Kalakkunnath, S.; Kalika, D. S. *Macromolecules* **2005**, *38*, 8381–8393.
- (23) Lin, H.; Freeman, B. D. *Macromolecules*, in press, 2005.
- (24) Stern, S. A.; Mullhaupt, J. T.; Gareis, P. J. *AIChE J.* **1969**, *15*, 64–73.
- (25) *DIPPR Physical and Thermodynamic Properties*; <http://dippr.byu.edu/public/chemsearch.asp>.
- (26) Freeman, B. D. In *Comprehensive Polymer Science: First Supplement*; Aggarwal, S. L., Russo, S., Eds.; Pergamon Press: New York, 1992; pp 167–98.
- (27) Bondar, V. I.; Freeman, B. D.; Pinnau, I. *J. Polym. Sci., Part B: Polym. Phys.* **1999**, *37*, 2463–75.
- (28) Koros, W. J.; Paul, D. R. *J. Polym. Sci., Part B: Polym. Phys. Ed.* **1976**, *14*, 1903–7.
- (29) Lin, H.; Freeman, B. D. In *Springer-Handbook of Materials Measurement Methods*; Czichos, H., Smith, L. E., Saito, T., Eds.; in press, 2005.
- (30) Prabhakar, R. S.; Raharjo, R.; Toy, L. G.; Lin, H.; Freeman, B. D. *Ind. Eng. Chem. Res.* **2005**, *44*, 1547–56.
- (31) Schuld, N.; Wolf, B. A. In *Polymer Handbook*; Brandrup, J., Immergut, E. H., Grulke, E. A., Eds.; John Wiley & Sons: New York, 1999; pp VII 247–64.
- (32) Kamiya, Y.; Naito, Y.; Mizoguchi, K.; Terada, K.; Mortimer, G. A. *J. Polym. Sci., Part B: Polym. Phys.* **1997**, *35*, 1049–53.
- (33) Bevington, P. R.; Robinson, D. K. *Data Reduction and Error Analysis for the Physical Sciences*, 2nd ed.; McGraw-Hill: New York, 1992.
- (34) Sperling, L. H. *Introduction to Physical Polymer Science*, 3rd ed.; Wiley-Interscience: New York, 2001.
- (35) Suwandi, M. S.; Stern, S. A. *J. Polym. Sci., Part B: Polym. Phys.* **1973**, *11*, 663–81.
- (36) Young, R. J.; Lovell, P. A. *Introduction to Polymers*, 2nd ed.; Chapman & Hall: London, U.K., 1991.
- (37) Hildebrand, J. H.; Prausnitz, J. M.; Scott, R. L. *Regular and Related Solutions: The Solubility of Gases, Liquids, and Solids*; Van Nostrand Reinhold Company: New York, 1970.
- (38) Prausnitz, J. M.; Lichtenthaler, R. N.; de Azevedo, E. G. *Molecular Thermodynamics of Fluid-Phase Equilibria*, 3rd ed.; Prentice Hall: New Jersey, 1999.
- (39) Michaels, A. S.; Bixler, H. J. *J. Polym. Sci.* **1961**, *50*, 393–412.
- (40) Merkel, T. C.; Bondar, V. I.; Nagai, K.; Freeman, B. D.; Pinnau, I. *J. Polym. Sci., Part B: Polym. Phys.* **2000**, *38*, 415–34.
- (41) Kamiya, Y.; Naito, Y.; Terada, K.; Mizoguchi, K. *Macromolecules* **2000**, *33*, 3111–9.
- (42) Van Krevelen, D. W. *Properties of Polymers: Their Correlation with Chemical Structure, Their Numerical Estimation and Prediction from Additive Group Contributions*; Elsevier: Amsterdam, 1990.
- (43) Dhoot, S. N.; Freeman, B. D.; Stewart, M. E.; Hill, A. J. *J. Polym. Sci., Part B: Polym. Phys.* **2001**, *39*, 1160–72.
- (44) Prabhakar, R. S.; Freeman, B. D.; Roman, I. *Macromolecules* **2004**, *37*, 7688–97.
- (45) Gee, G. *Quart. Rev.* **1947**, *1*, 265–98.
- (46) Barrer, R. M.; Skirrow, G. *J. Polym. Sci.* **1948**, *3*, 564–75.
- (47) Bondar, V. I.; Freeman, B. D.; Yampolskii, Y. P. *Macromolecules* **1999**, *32*, 6163–72.
- (48) Stiel, L. I.; Chang, D.; Chu, H.; Han, C. D. *J. Appl. Polym. Sci.* **1985**, *30*, 1145–65.
- (49) Tseng, H.; Wong, P.; Lloyd, D. R.; Barlow, J. W. *Polym. Eng. Sci.* **1987**, *27*, 1141–7.
- (50) Stiel, L. I.; Harnish, D. F. *AIChE J.* **1976**, *22*, 117–22.
- (51) Yampolskii, Y. P.; Soloviev, S. A.; Gringolts, M. L. *Polymer* **2004**, *45*, 6945–52.
- (52) Merkel, T. C.; Bondar, V.; Nagai, K.; Freeman, B. D.; Yampolskii, Y. P. *Macromolecules* **1999**, *32*, 8427–40.
- (53) Alentiev, A. Y.; Shantarovich, V. P.; Merkel, T. C.; Bondar, V. I.; Freeman, B. D.; Yampolskii, Y. P. *Macromolecules* **2002**, *35*, 9513–22.
- (54) Tseng, H.; Lloyd, D. R.; Ward, T. C. *Polym. Commun.* **1984**, *25*, 262–5.
- (55) Sanchez, I. C.; Rodgers, P. A. *Pure Appl. Chem.* **1990**, *62*, 2107–14.

- (56) Prabhakar, R. S.; Merkel, T. C.; Freeman, B. D.; Imizu, T.; Higuchi, A. *Macromolecules* **2005**, *38*, 1899–910.
- (57) Chandak, M. V.; Lin, Y. S.; Ji, W.; Higgins, R. J. *J. Appl. Polym. Sci.* **1998**, *67*, 165–75.
- (58) Flory, P. J. *Principles of Polymer Chemistry*; Cornell University Press: Ithaca, NY, 1953.
- (59) Fogg, P. G. T.; Gerrard, W. *Solubility of Gases in Liquids*; Wiley: New York, 1991.
- (60) Gibanel, F.; Lopez, M. C.; Royo, F. M.; Santafe, J.; Urieta, J. S. *J. Solution Chem.* **1993**, *22*, 211–7.
- (61) Myers, A. W.; Rogers, C. E.; Stannett, V.; Szwarc, M. *Mod. Plast.* **1957**, 157–65.
- (62) Mogri, Z.; Paul, D. R. *Polymer* **2001**, *42*, 7781–9.
- (63) Cowling, R.; Park, G. S. *J. Membr. Sci.* **1979**, *5*, 199–207.
- (64) Lin, H.; Shenogin, S.; Nazarenko, S. *Polymer* **2002**, *43*, 4733–43.
- (65) Puleo, A. C.; Paul, D. R.; Wong, P. K. *Polymer* **1989**, *30*, 1357–66.
- (66) Lasoski, S. W.; Cobbs, W. H. *J. Polym. Sci.* **1959**, *36*, 21–33.
- (67) Lowell, P. N.; McCrum, N. G. *J. Polym. Sci., Part A-2* **1971**, *9*, 1935–54.
- (68) Alter, H. *J. Polym. Sci.* **1962**, *57*, 925–35.
- (69) Polyakova, A.; Stepanov, E. V.; Schiraldi, D. A.; Hiltner, A.; Baer, E. *J. Polym. Sci., Part B: Polym. Phys.* **2001**, *39*, 1911–19.
- (70) Wierzchowski, S. J.; Kofke, D. A. *J. Phys. Chem. B* **2003**, *107*, 12808–13.
- (71) Dymond, J. H.; Smith, E. B. *The Virial Coefficients of Pure Gases and Mixtures: A Critical Compilation*; Oxford University Press: New York, 1980.
- (72) Reid, R. C.; Prausnitz, J. M.; Poling, B. E. *The Properties of Gases and Liquids*; McGraw-Hill: New York, 1987.

MA051218E